



An Optimal Control Technique for Single-Phase Grid-Connected Inverter

M. H. Ali¹, A. A. Sisa^{1,*}, A. B. Ahmed²

¹Department of Physics, Bayero University Kano, Kano, NIGERIA

^{2,3}Department of Physics, Gombe State University, Gombe, NIGERIA.

Abstract

This paper evaluates the performance of control technique based on Digital Pulse Width Modulation (DPWM) for single-phase grid-connected inverter application. Despite the importance of this synchronization technique, reports on its performance are scarce. The evaluation takes place in two simulation environments: ModelSim and MATLAB/Simulink. The performance of the technique expressed in Total Harmonic Distortion (THD) of Point of Common Coupling (PCC) current of the inverter is found to be 3.62%, a very good result on the standard of IEEE-519. This encouraging performance of this technique will result in injecting more renewable energy into the grid system, resulting in a more sustainable system.

Keywords: Renewable Energy Sources, Photovoltaic System, Grid-Connected Inverters, Model-Based Design, Simulink, ModelSim, Total harmonic distortion.

1.0 INTRODUCTION

Renewable Energy Sources (RES) such as wind, solar and hydro are now popular options to reducing the world's dependence on fossil-based fuels, which are known to deplete sooner or later [1]. Due to fast growth of Photovoltaic systems (PVS) installation; in upcoming years it will dominate the primary source of electric power [2]. The proper operation of grid-connected PVS depends largely on the efficiency of the Voltage Source Inverter (VSI). Important improvements in the design and implementation of the VSI can be carried out through the control of active and reactive power integration into the grid, reduction of the harmonic distortion, grid synchronization and digital implementation of the Grid-Connected Inverter (GCI) control [2].

The increasing demand for integration of PVS with the utility grid present challenges to improve system flexibility of GCI [3]. The efficiency of the grid-connected PVS mainly depends on the fast and accurate design of the GCI control system [4]. The stability and harmonics of the GCI are seriously affected by the uncertainties of the utility grid at the Point of Common Coupling (PCC), this is due to the power distortion introduced by the connected inverters

and non-linear load to the grid. Digital Pulse Width Modulation (DPWM) technique is mainly adopted for controlling the GCI, which injects power into the grid with less distortion [5].

DPWM as a control mechanism for GCI has an advantage of its ability to reduce the low order harmonic components of sinusoidal signals [4]. This is achievable by comparing a triangular carrier signal having high frequency with a low frequency sinusoidal reference signal, the point intersection between the signal determines the switching pulses that drive the gates of the VSI [6]. Research efforts have been made on the viability of integrating PVS with the utility grid. Most of the research mainly focused on the GCI control technique in order to inject high quality power to the grid with less distortion [7–10]. The work of [11] proposed control technique based on DPWM to synchronize a sinusoidal output voltage of the utility grid. Their technique also control the power injected to the utility grid to minimize distortion, by adopting simulation using PSIM [4]. It must be pointed out that the performance of DPWM technique to synchronize grid parameters when the current and voltage wave forms are distorted at the PCC is not adequately reported in the literature despite its popularity.

In this work, we evaluated the performance of DPWM synchronization technique for single-phase grid-connected inverter under adverse grid condition. To verify the effectiveness of this technique, harmonic analysis was performed and the result obtained was compared with the International Standard.

*Corresponding author (Tel: +234 (0) 8036408923)

Email addresses: mutariali@gmail.com (M. H.

Ali), sisa@gsu.edu.ng (A. A. Sisa), garkuwaz@yahoo.com (A.B. Ahmed)

This paper is structured in five sections: Section 1 is an introduction. Section 2 provides a brief theoretical background of the research. Section 3 describe modelling adopted. Section 4 is reserved to the simulation and co-simulation results found. Finally, a main conclusion of this work is drawn in section 5.

2.0 THEORETICAL BACKGROUND

The basis of Grid-Connected PVS (GCPVS) control is achievable by the adjustment of the amplitude, phase and frequency between the inverter and the grid voltage and simultaneously controlling the power factor, with less distortion [10]. A typical circuit configuration of the GCPVS is presented in Figure 1, showing the digital control of the system. While Figure 2 illustrate phasor representation of the equivalent electrical circuit of the inverter connected to the grid.

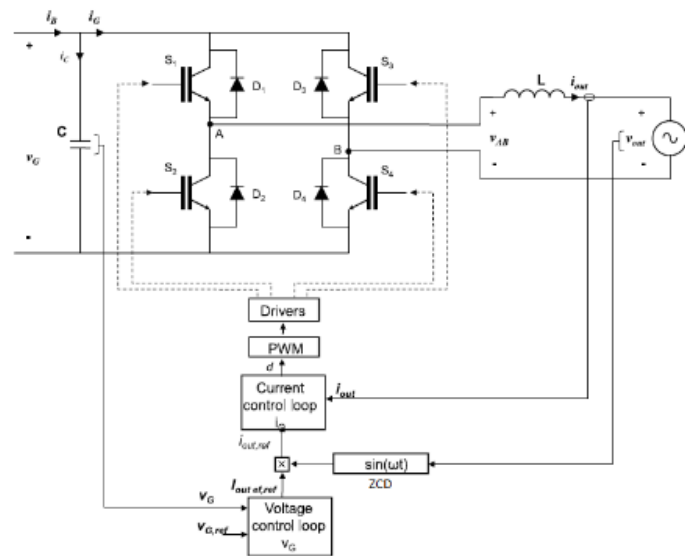


Figure 1: Circuit configuration of the grid-connected PVS with digital control [4]

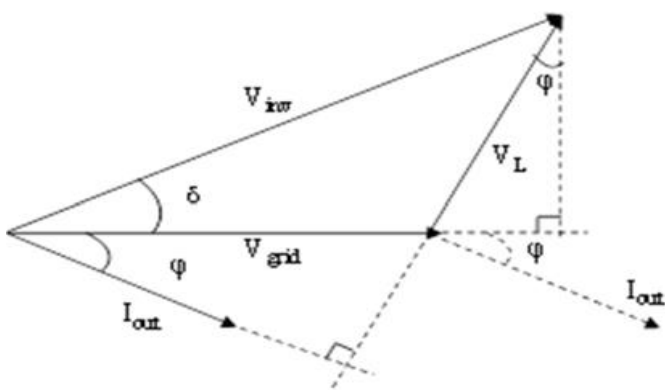


Figure 2: Phasor representation of the equivalent electrical circuit of the inverter connected to the grid [11]

The power control is obtained by means of the phase shift angle (δ) of the inverter output voltage, with respect to the grid voltage and the use of DPWM patterns. The power factor is determined by angle (φ) between the grid voltage and the fundamental current component of the inverter. By controlling the phase shift of the inverter output voltage and current, the amplitude and the power factor can be controlled. Thus, result in the control of magnitude of the active and reactive power integrated into the grid [12].

To simplify the design procedure, the single-phase voltage signal is considered to be as in equation (i) [13].

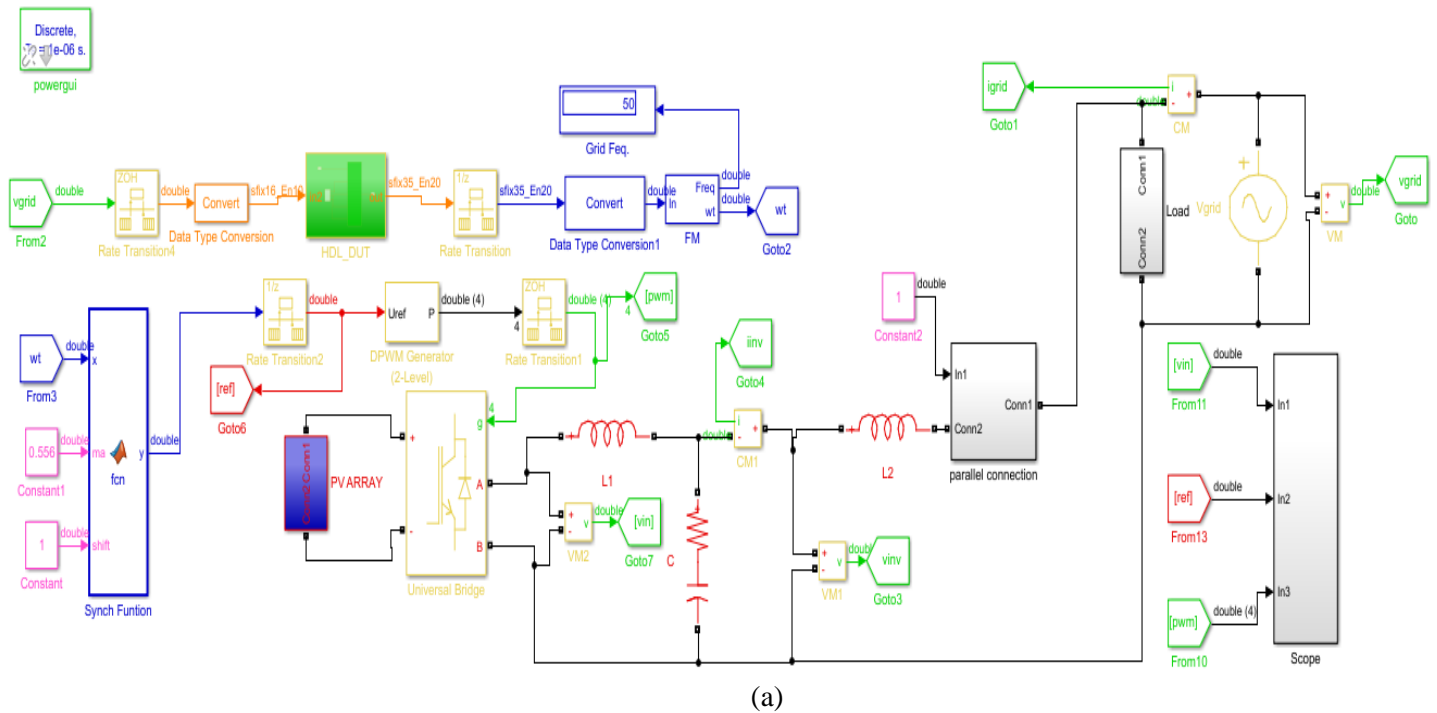
$$v(t) = v_1(t) + v_h(t) \tag{i}$$

Such that,

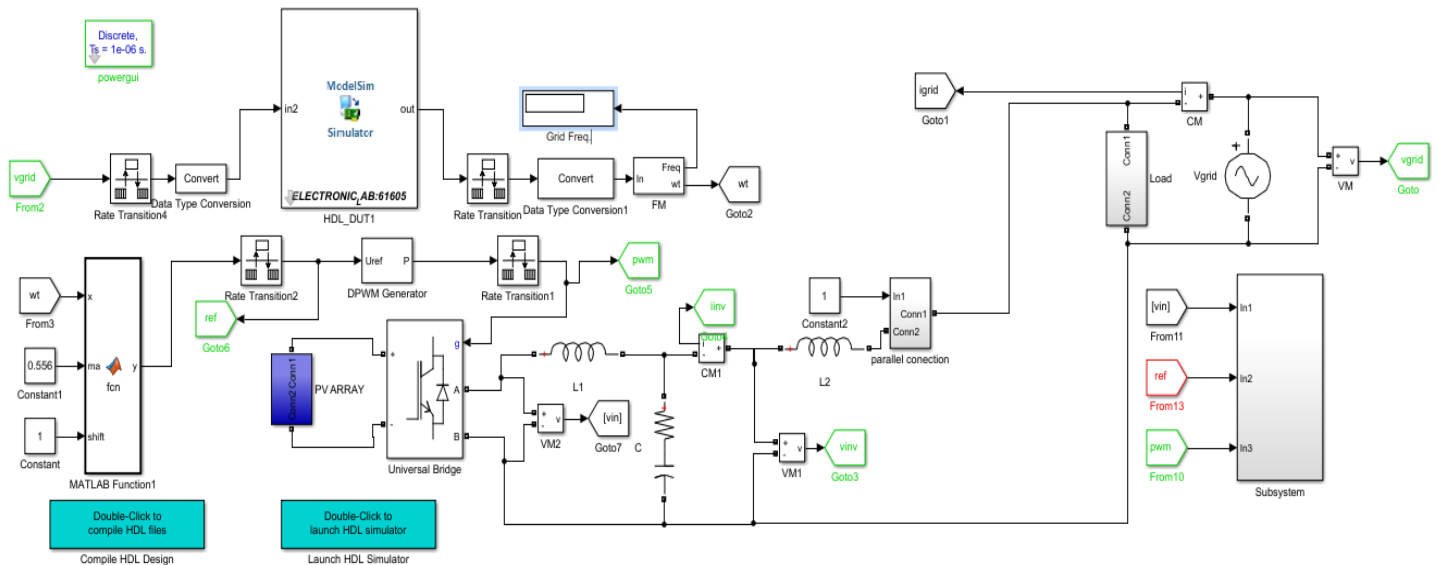
$$v(t) = V_1 \sin(\theta_1) + V_h \sin(\theta_h) \tag{ii}$$

where $v_1(t)$ is the fundamental component and $v_h(t)$ is h^{th} harmonic component in the single-phase voltage signal, and θ_1 and V_1 are the phase angle and amplitude of the fundamental component while θ_h and V_h are the phase angle and amplitude h^{th} harmonic component. Here, for the sake of simplicity, θ_1 and θ_h are defined as $\theta_1 = \omega_g t + \varphi_1$ and $\theta_h = \omega_g t + \varphi_h$ where ω_g is the fundamental angular frequency and φ_1 and φ_h are initial phase angles. Considering the fundamental harmonic of a pure sinusoidal wave, as a first approach, the total harmonics (THD) of the current injected into the grid is equal zero.

The GCPVS have to operate within a pre-defined power quality standard. IEEE-519 and IEC-61000-6-3 are the widely accepted standards that define the power quality and harmonic distortion limits for the electric power grid [14]. Frequency modulation index and the displacement factor have to be within the pre-calculated limits to guarantee undistorted output voltage and current. This magnitude can be controlled by selecting an adequate amplitude modulation index, and a phase shift angle of the inverter output voltage. To evaluate performance of the system based on distortion of the inverter current and voltage waveform, Total Harmonic Distortion (THD) is often used [7]. According to IEEE 519, THD is the ratio of the root-mean-square of the harmonic content to the root-mean-square value of the fundamental quantity and expressed as a percent of the fundamental value. The optimization equations for THD of voltage at the PCC and that of current are given in (iii) and (iv) [3].



(a)



(b)

Figure 3: Grid-connected PV system Model with Control (a) Simulation Model with SIMULINK (b) Co-simulation model with ModelSim.

$$\%THD_{V_{pcc}} = \frac{\sqrt{\sum_{h=2}^{\infty} V_{pcc}^2}}{V_1} \times 100 \quad (iii)$$

$$\%THD_i = \frac{\sqrt{\sum_{h=2}^{\infty} i_h^2}}{I_1} \times 100 \quad (iv)$$

where the V_1 and I_1 is the magnitude voltage and current of the fundamental component of the frequency spectrum while $\sqrt{\sum_{h=2}^{\infty} V_{pcc}^2}$ and $\sqrt{\sum_{h=2}^{\infty} i_h^2}$ is the magnitude or RMS value of harmonic components.

3.0 METHOD

This work was carried out using Model-Based Design workflow in two approaches: In the first approach

simulation was adopted using Simulink and for the second approach, a co-simulation test bench with the Simulink model of the GCPVS was adopted using ModelSim (Hardware Description Language simulator).

The two-level VSI regulates DC bus voltage at 400 V of the PV array and keeps unity power factor. The control system uses two control loops: the input side control loop which regulates DC link voltage to ± 400 V and grid side control loop which synchronized the grid parameter and regulate power injected to the grid using DPWM to reduce power distortion [11]. The grid voltage V_g is extracted and a reference signal U_{ref} is generated which is used by the DPWM two-level pulse generator to drive the gates of the VSI. The control system uses a sample time of $100\mu s$ for voltage and current controllers as well as zero crossing detector used for the synchronization unit. Detailed model of pulse generators of VSI uses a fast sample time of $1\mu s$ in order to get an appropriate resolution of PWM waveforms. The circuit configuration in Figure 1 is modeled in the Simulink environment as shown in Figure 3 (a) while a co-simulation model is shown in Figure 3 (b).

Both models are made up of the PV array and number of peripheral modules, such as the filters, inversion and control technologies. The system does not require storage system as they operate in parallel with the electric utility grid. In addition, they supply power back to the utility grid when the power generated by the GCPVS is greater than the load demand. And it receives power from the utility grid when power generated by the GCPVS is less than the load demand.

4.0 RESULTS AND DISCUSSION

The single-phase grid-connected inverter; Digital Pulse-Width-Modulator (DPWM) and its behavioural control have been simulated and verified. The basic parameters used for simulation and co-simulations in Figure 3 are $V_g = 220$ V, frequency = 50Hz, $L = 20.7$ mH and $V_{dc} = 400$ V. The DPWM converts the code in pulsating signal and generates the driving signals of the switches. Figure (4) through (7) shows the results of the grid-connected PVS modeled in Simulink environment. Figure (4) show the digital implementation of the DPWM for the simulink model. The graph in Figure (5) shows the DC voltage, the grid voltage and the synchronized grid and inverter current at the PCC. Figure (6) shows the grid and inverter output voltage, the synchronized grid voltage and current and the synchronized inverter voltage and currents. Figure (7) show

the harmonic analysis conducted on the PCC current of the inverter from which %THD was obtained.

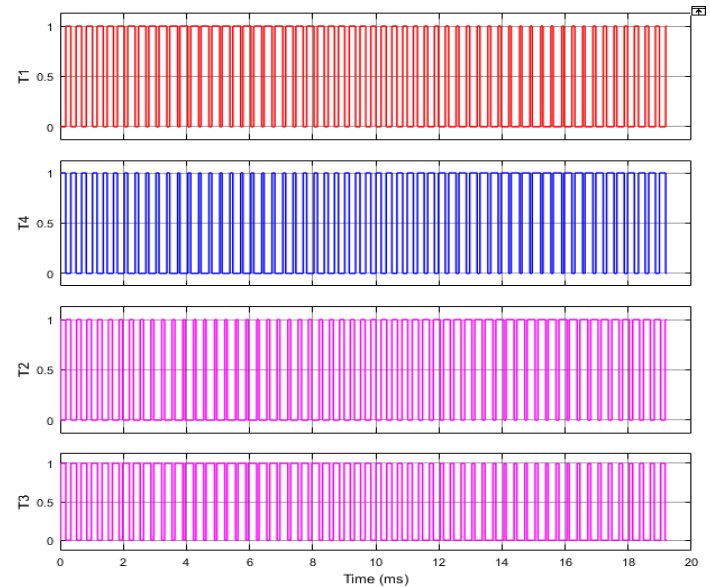


Figure 4: DPWM signal for Simulink

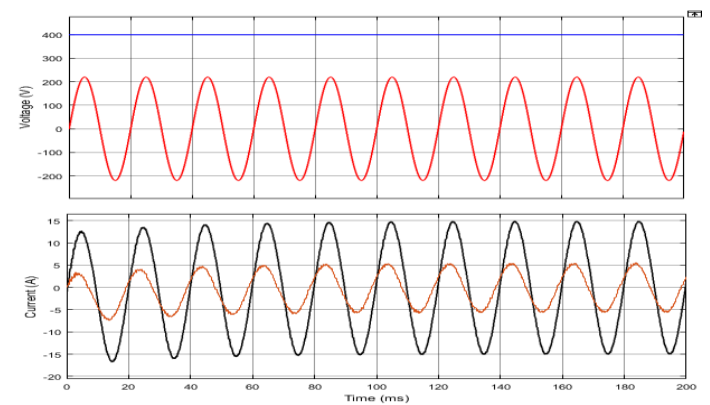


Figure 5: DC voltage, grid Voltage, grid output current and inverter output current for Simulink

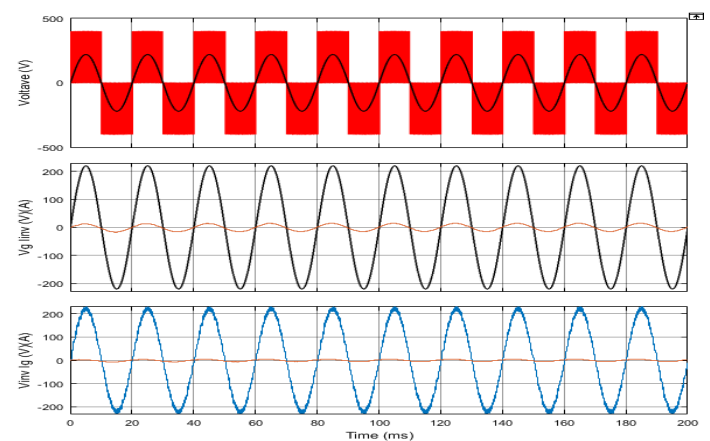


Figure 6: Inverter output voltage, grid voltage, Synchronized grid voltage, synchronized inverter voltage and currents for Simulink

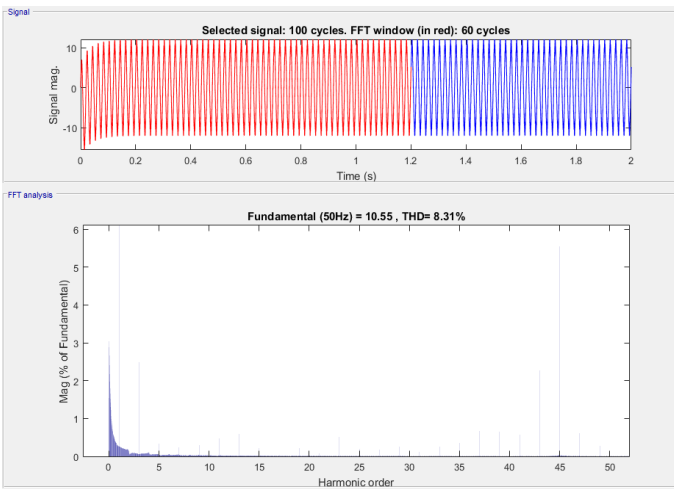


Figure 7: FFT analyses of PCC current of inverter for Simulink Model

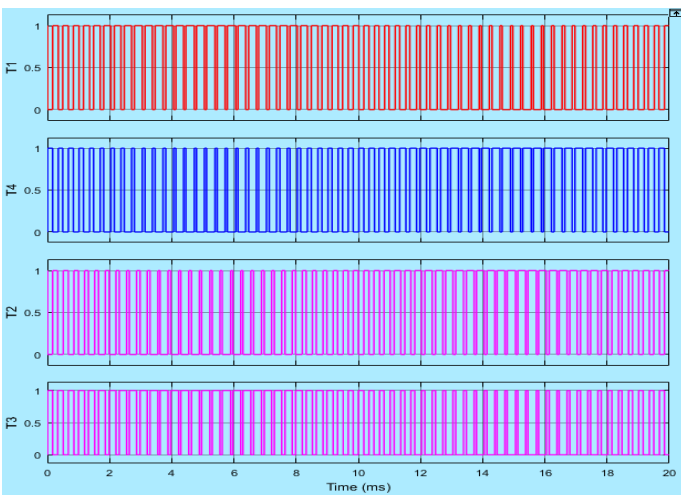


Figure 8: DPWM signal for Simulink for co-simulation in Mode Sim

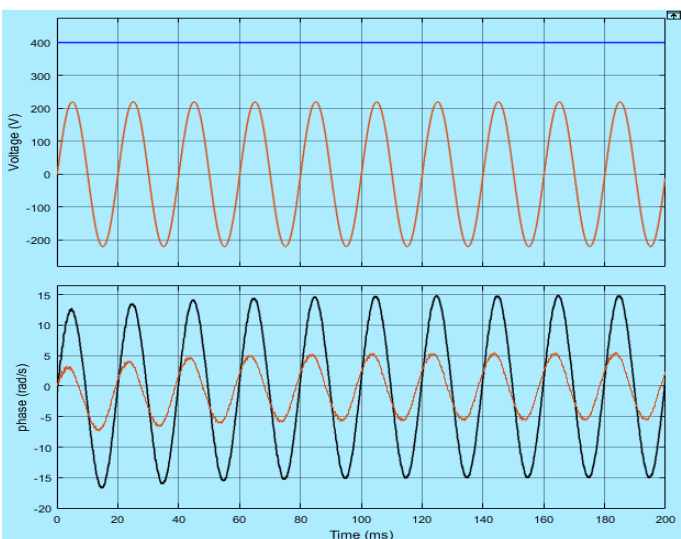


Figure 9: DC voltage, grid Voltage, grid output current and inverter output current for co-simulation model in ModelSim

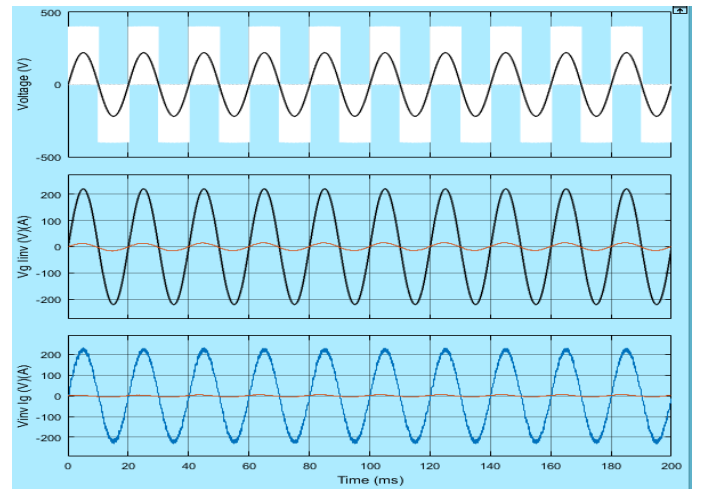


Figure 10: Inverter output voltage, grid voltage, Synchronized grid voltage, synchronized inverter voltage and currents for co-simulation model

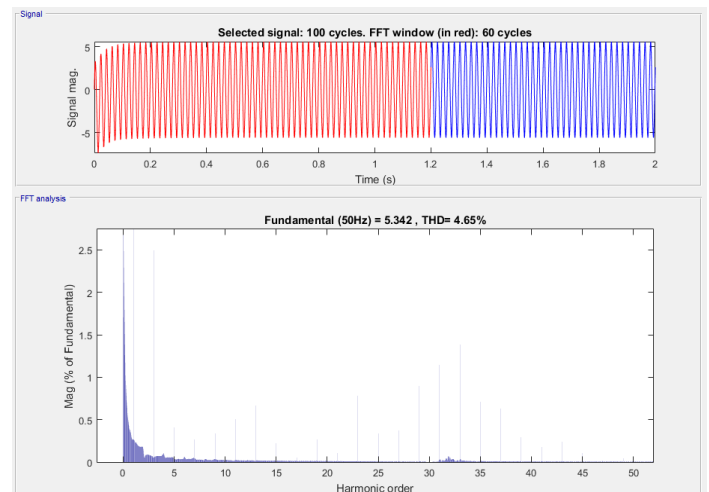


Figure 11: FFT analyses of PCC current of inverter for co-simulation Model

Figure (8) through (11) shows the results of the grid-connected PVS modeled with Simulink and co-simulated with ModelSim to test the optimized Hardware Description Language (HDL) code generated from the MATLAB/Simulink. Figure (8) shows the digital implementation of the build code of DPWM co-simulated with the ModelSim. Figure (9) shows the DC voltage, the grid voltage and Synchronized grid and inverter current at the PCC. Figure (10) shows the grid and inverter output voltage, the synchronized grid voltage and current and the synchronized inverter voltage and currents. Figure (11) show the harmonic analysis conducted on the PCC current of the inverter in the co-simulated model from which %THD was obtained.

It can be observed from Figure (5) and (9) that the DC link voltage was maintained constant at about 400V for both the models, and also there is synchronization in grid

and inverter current at the PCC. From Figure (6) and (10). It can also be seen that there is synchronization in the grid voltage and inverter current and Vice Versa, which is a requirement for injection power to the grid. It was very difficult to study distorted waveform viewed in time domain, as such the signal were expressed as the summation of series of sinusoidal waveforms with varying magnitudes and frequencies using Fourier Series [15]. The magnitude and frequency of each sinusoidal signal were then plotted to view the distorted time-domain signal on a frequency domain using Fast Fourier Transform (FFT)[3].

In the harmonic analysis conducted on the inverter current presented in Figure (7) and (11), %THD was found to be 8.31% and 4.65% for the Simulink and co-simulation models respectively. Also %THD was evaluated using equation (iii) and (iv) which was obtained to be 6.76% and 3.62% for Simulink and co-simulation model respectively. The calculated and FFT analysis values for %THD are presented in Table 1. From the result it can be seen that the THD is reduced when the HDL code was optimised by the HDL simulator (ModelSim).

Table 1: Harmonic analysis of inverter current

S/ N	Approach	Inverter	
		Current %THD (Calculated)	Inverter Current %THD (FFT analysis)
1	Simulation	6.76	8.31
2	Co-Simulation	3.62	4.65

5.0 CONCLUSION

We found the total harmonic distortion of point of coupling current of the inverter to be 3.62%. This result is very good since it is not up to the maximum value of 5%; the specified limit for total harmonic distortion at the point of common coupling as prescribed by the IEEE-519 Standard. Thus, performance of this control technique; digital pulse width modulation suggested it can facilitate the successful synchronization of the inverter and the utility grid power. This will enable integration of large amount of power from grid connected inverters into the utility grid leading to injection of adequate power for the community consumptions.

REFERENCES

[1] M. H. Ali and I. G. Abdulsalam, "Determination of Cloud Effect on the Performance of Photovoltaic Module," IOSR Journal of Electrical and Electronics

Engineering, 8(4), pp. 03–07, 2016, doi: 10.9790/4861-0804020307.

- [2] E. Kabalc, "Review on Novel Single-Phase Grid-Connected Solar Inverters: Circuits and Control Methods," vol. 198, no. October 2019, pp. 247–274, 2020, doi: 10.1016/j.solener.2020.01.063.
- [3] J. Xu, Q. Qian, B. Zhang, and S. Xie, "Harmonics and Stability Analysis of Single-Phase Grid-Connected Inverters in Distributed Power Generation Systems Considering Phase-Locked Loop Impact" Institute of Electrical and Electronics Engineers Transactions on Sustainable Energy, vol. 10, no. 3, pp. 1470–1480, 2019, doi: 10.1109/TSTE.2019.2893679.
- [4] L. Hassaine and M. R. Bengourina, "Control technique for single phase inverter photovoltaic system connected to the grid," Energy Reports, 6, September 2019, pp. 200–208, 2020, doi: 10.1016/j.egyr.2019.10.038.
- [5] Zeb et al., "A comprehensive review on inverter topologies and control strategies for grid connected photovoltaic system," Renewable and Sustainable Energy Reviews, 94, pp. 1120–1141, 2018, doi: 10.1016/j.rser.2018.06.053.
- [6] D. B. N. Nnadi, S. E. Oti, and C. I. Odeh, "Cascaded Single-Phase, Pwm Multilevel Inverter with Boosted Output Voltage," *Nigerian Journal of Technology*, 39(2), pp. 589–599, 2020.
- [7] L. Hassaine and M. R. Bengourina, "Design and digital implementation of power control strategy for grid connected photovoltaic inverter," *International Journal of Power Electronics and Drive Systems* 10(3), pp. 1564–1574, 2019, doi: 10.11591/ijpeds.v10.i3.1564-1574.
- [8] C. Dang, X. Tong, and W. Song, "Sliding-mode control in dq-frame for a three-phase grid-connected inverter with LCL-filter," *Journal of the Franklin Institute*, 357, 15, pp. 10159–10174, 2020, doi: 10.1016/j.jfranklin.2019.12.022.
- [9] A. Safa, E. L. Madjid Berkouk, Y. Messlem, and A. Gouichiche, "A robust control algorithm for a multifunctional grid tied inverter to enhance the power quality of a microgrid under unbalanced conditions", *International Journal of Electrical Power & Energy Systems*, 100, February, pp. 253–264, 2018, doi: 10.1016/j.ijepes.2018.02.042.
- [10] Y. Yongheng and B. Frede, "Overview of Single-Phase Grid-Connected Photovoltaic Systems," *Electric Power Components and Systems*, 43(12), pp. 1352–1363, 2015.
- [11] L. Hassaine and A. Mraoui, "Control strategy based on SPWM switching patterns for grid connected

- photovoltaic inverter,” *AIP Conference Proceedings*, 1814(4), 2017, doi: 10.1063/1.4976250.
- [12] L. Hassaine and M. R. Bengourina, “Design and control technique for single phase bipolar H-bridge inverter connected to the grid,” *International Journal of Electrical and Computer Engineering*, 10(3), pp. 3057–3065, 2020, doi: 10.11591/ijece.v10i3.pp3057-3065.
- [13] H. Sepahvand, M. Saniei, S. S. Mortazavi, and S. Golestan, “Performance Improvement of Single-Phase PLLs Under Adverse Grid Conditions: An FIR Filtering-Based Approach,” *Electric Power Systems Research*, 190, no. August 2020, p. 106829, 2021, doi: 10.1016/j.epsr.2020.106829.
- [14] IEEE Std 519, “IEEE Std 519-2014 (Revision of IEEE Std 519-1992), IEEE Recommended Practice and Requirements for Harmonic Control in Electric Power Systems,” IEEE Std 519-2014 (Revision of *Institute of Electrical and Electronics Engineers Std 519-1992*), vol. 2014, pp. 1–29, 2014, [Online]. Available: <http://ieeexplore.ieee.org/servlet/opac?punumber=6826457>.
- [15] A. A. Sisa, M. H. Ali, and Z. Sagir, “A Novel Finite Impulse Response Filter Design using Windowing,” *Journal of the Nigerian Association of Mathematical Physics*, 46(2), pp. 15–27, 2018.